Cellular DNA Methylation Program during Neurulation and its Alteration by Alcohol Exposure

Feng C. Zhou,* Yuanyuan Chen, and Ada Love
Department of Anatomy & Cell Biology, Stark Neuroscience Research Institute, Indiana University School of Medicine. Indianapolis, Indiana

Received 15 November 2010; Revised 25 February 2011; Accepted 4 March 2011

BACKGROUND: Epigenetic changes are believed to be among the earliest key regulators for cell fate and embryonic development. To support this premise, it is important to understand whether or not systemic epigenetic changes coordinate with the progression of development. We have demonstrated that DNA methylation is programmed when neural stem cells differentiate (Zhou et al., 2011). Here, we analyzed the DNA methylation events that occur during early neural tube development. **METHODS AND RESULTS:** Using immunocytochemistry, we demonstrated that the DNA methylation marks – 5-methylcytosine (5-MeC), DNA methylation binding domain 1 (MBD1), and DNA methytransferases 1 (DNMT1) were highly coordinated in temporal and spatial patterns that paralleled the progress of embryonic development. The above ontogenic program of DNA methylation was, however, subjected to environmental modification. Alcohol exposure during fetal development, which is known to cause fetal alcohol spectrum disorder, altered the density and distribution of the DNA methylation marks. The alcohol exposure (88 mM) over 6 or 44 hours at gestation day 8 (GD-8) to GD-10 altered timely DNA methylation and retarded embryonic growth. We further demonstrated that the direct inhibiting of DNA methylation with 5-aza-cytidine (5-AZA) resulted in similar growth retardation. **CONCLUSIONS:** We identified a temporal and spatial cellular DNA methylation program after initial erasure, which parallels embryonic maturation. Alcohol delayed the cellular DNA methylation program and also retarded embryonic growth. Since direct inhibiting of DNA methylation resulted in similar retardation, alcohol thus can affect embryonic development through a epigenetic pathway. *Birth Defects Research (Part A) 00:000–000, 2011.* © 2011 Wiley-Liss, Inc.

Key words: epigenetics; MBD1; DNMT; differentiation; fetal alcohol syndrome; neural tube; neural crest

INTRODUCTION

Epigenetics, including the methyl marks on the top of DNA and histone that are associated with chromatin configuration, allow accessibility of the regulatory binding protein for gene transcription. DNA methylation at the CpG dinucleotide represents an important regulatory component of mammalian genomes. The cytosine of this dinucleotide serves as the target for methylation via the action of DNA methyltransferases (DNMT). Methylated DNA is correlated with transcriptionally inactive genes, whereas actively expressed genes are generally hypomethylated (Bird, 1987; Singal and Ginder, 1999). It has also been suggested that cytosine methylation represents a defense mechanism that silences the parasitic repetitive DNA elements, including transposons present in mammalian genomes (Walsh and Bestor, 1999). Cytosine methylation also plays an important role in (1) the process of genomic imprinting, in which paternal and maternal alleles of a gene exhibit distinct patterns of methylation and expression (Tilghman, 1999), and (2) X-chromosome inactivation, in which one X-chromosome in each cell of a woman becomes transcriptionally inactivated during early development (Pfeifer et al., 1990). Appropriate cytosine methylation is essential for normal mammalian development. Individual ablation of the DNA methyltransferase genes DNMT1, DNMT3a, or DNMT3b leads to a disruption of murine embryonic development

This study was supported by RO1AA016698 and Alcohol Center project P50 AA07611 (Feng C. Zhou). Dr. David Crabb is director of the Center project P50 AA07611. Yuanyuan Chen is supported in part by the Stark Neuroscience Research Institute fellowship.
*Correspondence to: Feng C. Zhou, Department of Anatomy & Cell Biology, Indiana University School of Medicine, Indianapolis, IN 46202. E-mail: imce100@iupui.edu
Published online in Wiley Online Library (wileyonlinelibrary.com).
DOI: 10.1002/bdra.20820

(Okano et al., 1999; Wu et al., 2010). Furthermore, mutations in DNMT3b that are predicted to partially inhibit function are associated with the immunodeficiency, centromere instability, and facial anomalies syndrome in humans (Hansen et al., 1999; Ueda et al., 2006). Also, mutations in the methyl-CpG-binding protein MeCP2 lead to Rett's syndrome, a progressive neurodegenerative disorder (Amir et al., 1999; Shahbazian and Zoghbi, 2002).

Because DNA methylation is modifiable and heritable during cell duplication, through the regulation of specific genes or clusters of genes, it plays an important role in the developmental stages, including germ cell imprinting (Bartolomei, 2003), stem cell maintenance (Cheng et al., 2005; Kondo, 2006; Zhang et al., 2006; Meshorer, 2007; Surani et al., 2007; Tang and Zhu, 2007), cell fate, and tissue patterning (Kiefer, 2007). Moreover, DNA methylation modification has been considered a program since the beginning of life, from the fertilized egg to the blastocyte stage (Morgan et al., 2005; Yamazaki et al., 2007). Epigenetic programming includes a period of erasure of the existing set of paternal and maternal derived DNA methylation during early embryogenesis (morula; Kafri et al., 1992) followed by a period of less understood DNA re-methylation in the somatic and germ lines. DNA re-methylation takes place bimodally between housekeeping genes and tissue-specific genes, thus, conferring specificity to the cells and heterogeneity of the tissue (Lange and Schneider, 2010). We have previously demonstrated that epigenetic marks are highly dynamic in neural stem cells when departing from quiescent and multipotent state into the migrating and differentiating stages. There is an initial overall hypomethylation, followed by re-methylation in a subpopulation of cells. There is also an increase of DNA methylation binding domain protein (MBD1), along with histone modification, during the process of differentiation (Singh et al., 2009). This dynamic change at the cellular level is accompanied by the dynamic change of DNA methylation at the epigenomic level. We recently demonstrated that genome-wide DNA methylation was programmed during the differentiation of neural stem cells in which many moderately methylated genes were reprogrammed and became hypo-methylated or hyper-methylated (Zhou et al., 2011). Many of these genes are tissue-specific and functionally related to neural development. To date, how DNA methylation progresses during embryonic development and what role this DNA methylation in embryonic development plays is unclear. Specifically, to date, cellular DNA methylation beyond the early morula up to the stage of tissue specification and organ formation is mostly unknown. How and if DNA methylation mediates embryonic differentiation at the stage of tissue differentiation and organ formation has not been demonstrated, which is a major area of investigation.

While studying the active formation of the nervous system at the stage of neurulation, we asked, ''How was DNA methylated in the neural tube and neural crest cells during differentiation?'' More specifically, we wanted to know, ''How does DNA methylation appear in renewing precursor cells versus differentiating neural cells in the neural tube?'' Here, we examined the DNA methylation marks 5-methylcytosine (5-MeC), along with the 5-MeC mark transfer enzyme DNMT1 and the 5-MeC functional binding protein DNA MBD1, immunocytochemically during embryonic neural tube development through embryonic days 8.25 (E8.25), E9.25, E10, E10.25, and E15 in C57BL6 mice. These marks were compared to the state of neural differentiation referenced by stem cell gene *Oct4*, or neural differentiation markers, nestin, Crabp 1 (cellular retinoic acid binding protein 1), and microtubule-associated protein 2 (MAP2). We reported here, for the first time, that DNA methylation was dynamically changed, and its change was closely associated with neural tube formation in a unique manner as a program.

We also asked if the normal DNA methylation program is subject to the input of an environmental factor. We have previously demonstrated that alcohol altered the DNA methylation of many genes in the embryos at the beginning of neurulation (Liu et al., 2009). Alcohol is a source of nutrition as well as a substance of abuse. Alcohol, furthermore, is a potent environmental factor, which has a major impact on epigenetics because it (1) affects the methyl donor through folic acid metabolism (LaBaume et al., 1987; Cravo and Camilo, 2000; Mason and Choi, 2005) and (2) can also prevent folic acid absorption at the systemic (Hamid et al., 2009) and cellular level (McGeer et al., 1983). Alcohol exposure to embryos has been shown to alter DNA methylation biochemically (Garro et al., 1991), at specific genes (Haycock, 2009), and on a genome-wide level (Liu et al., 2009). Women's abuse of alcohol during pregnancy often results in a broad array of physical and neurobiological defects, known as fetal alcohol spectrum disorders (FASD). Alcohol has been widely documented to interfere with embryonic development by affecting a cell's growth cell cycle, cell migration, or neuronal patterning and synaptic formation. The pathogenesis underlying the alcohol effect includes induced oxidative stress, defected adhesion molecules, and a lack of neurotrophic and developmental signaling (Goodlett et al., 2005). The mechanism underlining FASD is still unclear. Making a comparison with the normal cellular epigenetic program during neural tube formation, we also examined if epigenetic change occurred when exposed to alcohol in a whole embryo culture model at the stage of neurulation so we could investigate an alternative mechanism of FASD.

MATERIALS AND METHODS

Two-month-old C57BL/6 (B6) mice (~20 g; Harlan, Indianapolis, IN) were used. Mouse breeders were individually housed upon arrival and acclimated for at least 1 week before mating began. The mice were maintained on a 12 hour light–dark cycle (light on: 19:00–7:00) and provided laboratory chow and water ad libitum. Two female mice were placed with one male mouse for 1 hour. The mating time was 8:00 to 9:00. Many routine mating sets were used to ensure sufficient number of pregnancies. When a vaginal plug was detected after the mating period, it was designated as gestational day 0 (GD-0) or embryonic day 0 (E-0). On embryonic days E8.25, E8.5, E9.25, E10, and E15, dams were sacrificed by overdose using CO_2 gas. Then, embryos were harvested and fixed in 4% freshly prepared formaldehyde buffered with phosphate-buffered saline (PBS) for immunostaining of various DNA methylation marks and differentiation markers.

Whole Embryonic Culture

A subset of dams was used to analyze the effect of alcohol exposure. On E8.2 at 15:00, dams were sacrificed by overdose using CO_2 gas. The technique for the whole embryo culture was based on the method described by Dr. New (New, 1978) and our previous studies (Ogawa et al., 2005). Briefly, the gravid uterus was removed and placed in sterile PBS (0.1 M phosphate buffer containing saline) at 37°C. Leaving the visceral yolk sac and a small piece of the ectoplacental cone intact, the decidual tissues and the Reichert's membrane were removed carefully and immediately immersed in PBS that contained 4% fetal bovine serum (Sigma, St Louis, MO). Three embryos bearing 3 to 5 somites (E8.25) were placed in a culture bottle (20 mL) that contained the culture medium, which consisted of 70% immediately centrifuged heat-inactivated rat serum (Harlan Sprague–Dawley, Indianapolis, IN) and 30% PB1 buffer (137 mM NaCl, 2.7 mM KCl, 0.5 mM MgCl2, 8 mMNa2HPO4, 1.47 mM KH2PO4, 0.9 mM CaCl2, 5.6 mM glucose, 0.33 mM sodium pyruvate, and pH7.4). The embryos were then supplemented with penicillin and streptomycin (20 units/mL and 20 μg/mL, respectively (Sigma, St. Louis, MO). Bottles were gassed at 0 to 22 hours with 5% O_2, 5% CO_2, and 90% N_2, and at 22 to 44 hours with 20% O_2, 5% CO_2, and 75% N_2 in a rotating culture system (B.T.C. Precision Incubator Unit, B.T.C. Engineering, Cambridge, England, 36 revolutions per minute) at 37°C.

Alcohol treatment. After the pre-culture period (2–4 hours; maximum 4 hours), alcohol exposure was started by transferring the embryos into the medium containing 6 μL/mL of 95% ethanol for 6 or 44 hours. The control group was cultured in the medium with no ethanol. The culture medium was changed with fresh medium (the control or alcohol-medium treatments were changed according to the condition) per 24 hours. All cultures were terminated 44 hours from the beginning of the treatment. The concentration of ethanol in the medium was tested previously and peaked at 400 mg/dL (88 mM) at the presence of alcohol (Ogawa et al., 2005). The medium alcohol level used in the current study is comparable to the in vivo dosage of binge-like alcohol intake (Giknis et al., 1980; Wynter et al., 1983; Boehm et al., 1997). This level is considered within the range attained by human alcoholics (Hoffman, 1975; Lindblad and Olsson, 1976). A total of 60 embryos (control = 31, alcohol = 29 embryos) from 12 separate cultures were used in this study. In each culture, control embryos were included to avoid misevaluations that could have been produced by any differences in the cultural conditions among these experiments.

5-AZA-cytidine treatment. Two independent experiments with the DNA methylation inhibitor were performed in the embryonic culture used above: 6 hours 5-aza-cytidine (5-AZA) treatment study (control = 19, 5-AZA = 19 embryos) and 44 hours 5-AZA treatment study (control = 18, 5-AZA = 14 embryos). Along with a vehicle control, these included the 5-AZA (100 ng/mL) treatment instead of alcohol. These embryos were scored for their developmental staging (see below).

At the end of culture, all embryos were checked for their viability by confirming blood circulation of the yolk sac and the heart beating, before fixed in freshly prepared 4% formaldehyde in the PBS. Analysis of developmental staging using a scoring system, and analyses of methylation and differentiation markers using immunocytochemical staining are described in the sections below.

Morphologic Scoring

The embryonic growth scoring system was adapted from Brown and Fabro (1981) and Van Maele–Fabry et al. (1992), and used in our previous report (Ogawa et al., 2005). The forebrain, midbrain, hindbrain, heart, caudal neural tube, otic system, optic system, branchial bars, maxillary and mandibular processes, forelimb, and hindlimb were individually scored. A total score was given as a sum above the individual score. The somite number obtained a separate analysis. Non-parametric statistics were used for the morphologic scoring (embryonic growth) analysis because the scores represented an ordinal classification scale. Mann–Whitney *U* tests were used to test differences in each region of interest between the control and alcohol-treated embryos of each strain. To correct a type I error in the scoring analysis of the multiple analyses, the p values ≥ 0.0038 (0.05/13, indicated by *) and 0.0007 (0.01/13, indicated by **) were used to indicate the degree of statistical significance. Statistics were performed using Prism Software Version 4 (GraphPad Software, San Diego, CA). The 44 hours of alcohol treatment along with the vehicle controls were scored in this study.

Immunocytochemistry Analysis

Embryos of different gestations were embedded in gelatin singularly, sectioned in 40 micron, and processed for immunocytochemistry. The embryos of the two treatment groups were paired and embedded in gelatin together with careful alignment of their level and orientation. They were similarly sectioned and processed for immunocytochemistry in parallel; this practice avoids any bias through the staining procedure and is convenient for comparing levels of embryo sections side by side. All sections were then washed three times in PBS. They were then incubated in (1) 3% H_2O_2 (v/v) in PBS for 30 minutes and (2) PBS containing 4% normal control serum, and 0.3% Triton X-100 (TX) for 30 minutes at room temperature to block nonspecific binding. Sections were next incubated with antibodies against DNA methylation marks, 5-MeC (sheep polyclonal, 1:500, GeneTex, Irvine, CA), MBD1 (rabbit polyclonal, 1:500, Santa Cruz Biotechnology, Santa Cruz, CA), DNMT1 (goat polyclonal, 1:500, Santa Cruz Biotechnology) throughout E8.25 to E15, which allowed for developmental analysis. At E8.25 +6 hours or 44 hours, an analysis was conducted for alcohol effect. Antibodies for anti-MAP2 (goat, 1:400, Santa Cruz Biotechnology), anti-nestin (neuroepithelial marker, mouse, 1:500, BD Biosciences), anti-Crabp 1 (cellular retinoic acid binding protein 1, received from Dr. Wei, University of Missouri) were used for differentiation markers, mainly for embryos at E10.25. All primary antibodies were incubated overnight at room temperature. The sections were then incubated with a secondary antibody (1:250, Jackson ImmunoResearch Laboratory, West Grove, PA) for 1 hour, followed by an avidin-biotin peroxidase complex (Vector Laboratories) for 1 hour at room temperature. All sections were washed three times with PBS, 5 minutes each between each antibody incubation. The color reaction (brown) was developed by add-

ing 0.05% 3′ to 3′-diaminobenzidine tetrahydrochloride and 0.003% H_2O_2 in Tris buffer to reveal the peroxidase activity. All sections were counterstained with methyl green for a cellular profile.

Densitometry Analysis

For imaging, all pictures were taken using a Leitz Orthoplan2 microscope (Ernst Leitz GMBH, Wetzlar, Germany) with a Spot RT color camera (Diagnostic Instruments, Inc., Sterling Heights, MI). Bright-field images were taken with consistent setup and exposure time for each antibody staining. The outline of the cell is clearly distinguishable under the Leitz microscope at ×40 magnification. Immunostained images were converted to the 16-bit color format, and staining intensity was measured using Image J (National Institutes of Health, Bethesda, MD). Calibration was set based on 256 levels of the gray scale. A field of 130umX110um covering the region of interest was selected for analysis; each contained 80 to 120 cells. Each cell within the field was initially scored by their staining intensity (gray scale) as 0 (<30), 1 (30–60), 2 (60–90), 3 (90–120), or 4 (120–160), respectively. The number of cells stained at each intensity and the total number of cells in each field were counted first. An H-score was then calculated using the following formula adopted from Detre et al. (1995).

Immunostaining H-score = (% of cells that stained at intensity score 1 × 1) + (% of cells that stained at intensity score 2 × 2) + (% of cells that stained at intensity score 3 × 3) + (% of cells that stained at intensity score 4 × 4). (An H-score between 0 and 400 was obtained. The overall staining intensity was further ranked for illustration purpose in Table 1 and Figs. 1 and 2, where 0 indicates negative staining, ''+'' = 1–100, ''++'' = 101–200; ''+++'' = 201–300''; and ''++++'' = 301–400.)

Based on the H-score, Mann–Whitney *U* analysis was used to compare the two neural tube axial levels (i.e., caudal to hindbrain) or two regions within a neural tube (i.e., comparing ventral to dorsal neural tube at hindbrain level; Table 1).

The ventral neural tube was defined as the level from the floor plate to the alar plate of the neural tube; the dorsal neural tube, from the alar plate to the roof plate. The caudal neural tube referred to the neural tube from somite 22 to 28. The neural crest was measured at the region lateral to the neural tube (Fig. 1H).

For the analysis of alcohol's effect, bright field images were taken under ×10. Integrated density of marks in a region of the neural tube was measured by outlining the corresponding region of the neural tube. Images were converted into 16-bit in Image J as described above. Comparison of staining densities between alcohol-treated and control embryos were analyzed using a *t* test. For 5-MeC staining, 6 hour alcohol-treated embryos: n = 3; 44 hours alcohol-treated embryos: n = 4. For MBD1 staining, 6 hour alcohol treatment embryos: n = 4. All data were presented as Mean ± SEM. All statistics were done using Prism software Version4 (GraphPad Software, San Diego, CA).

RESULTS

Distribution of DNA-methylation Marks

The 5-MeC, MBD1, and DNMT1 were expressed in the embryo's developing organ, particularly in the neural tube and neural crest cells. A strikingly similar pattern of expression of the immunostained 5-MeC, MBD1, and DNMT1 was found in the neural tube, except in an early temporal pattern between 5-MeC and MBD1 (Table 1).

The 5-MeC-immunostaining (im) was distributed throughout the ectoderm, mesoderm, and endoderm with variable density at our earliest time point E8.25. In this report, however, we focused on the neural tube. The 5-MeC-im was distributed in a specific pattern in the developing neural tube. Two observations are new. First, in contrast to conventional understanding, all cells did not contain 5-MeC-im (Figs. 1 and 2), which shows that all DNA methylation are not instantaneously transmitted from parental to daughter cells. Second, there is a clear heterogeneous intranuclear distribution (Fig. 2A–C), as well as neural tube-wide distribution throughout the time course (Fig. 1), which demonstrates that there is a DNA methylation related to the chromatin dynamics within the cells and among the population during the neural tube development. The 5-MeC-im appeared first as a punctate (consolidated) form in the nucleus of the

Table 1
Semi-quantitation of 5-MeC-im and MBD1-im within neural tube, neural crest cells and blood cells in E9.25 to E10.25 embryos

		Forebrain NT		Hindbrain NT (ventral)		Hindbrain NT (dorsal)		Caudal NT		Neural crest cells	Blood cell
	Stage	H-score	Overall rank	H-score	Overall rank	H-score	Overall rank	H-score	Overall rank	H-score	H-score
5-MeC-im	E9.25	183 ± 9*	++	332 ± 5	++++	242 ± 10*	+++	191 ± 2*	++	+++	0
	E10	190 ± 11*	++	274 ± 23†	+++	210 ± 7*,†	+++	183 ± 2*,†	++	+++	0
	E10.25	190 ± 11*	++	297 ± 19	+++	229 ± 8*	+++	180 ± 19*	++	+++	0
MBD1-im	E9.25	137 ± 14*	++	323 ± 11	++++	214 ± 10*	+++	190 ± 12*	++	++++	0
	E10	183 ± 12*,†	++	310 ± 9	++++	184 ± 5*,†	++	200 ± 5*	++	+++	0
	E10.25	196 ± 9*,†	++	283 ± 2†	+++	270 ± 3†	+++	172 ± 16*	++	+++	0

5-MeC at each age: N = 3; MBD1 at each age: N = 4.
Mann–Whitney *U* nonparametric analysis. Data presented as mean ± SEM.
*$p < 0.05$ compare to hindbrain neural tube (ventral) at respective age.
†$p < 0.05$ compare to E9.25 stage in respective region.
5-MeC-im, 5-methylcytosine immunostaining; MBD1-im, methylation binding domain 1 immunostaining; NT, neural tube.

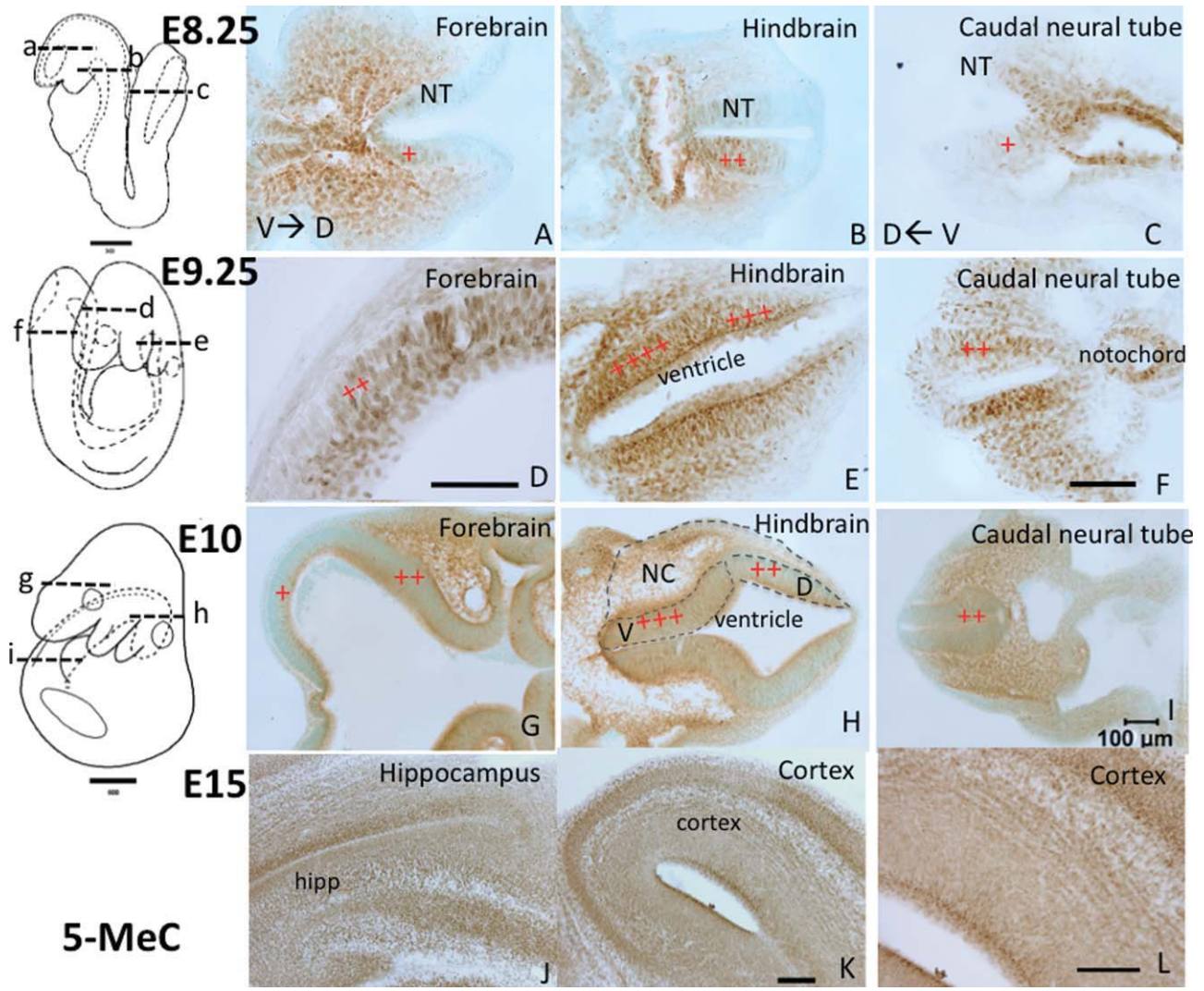

Figure 1. Spatial 5-MeC-immunostaining (im) distribution in neural tubes of E8.25 **(A–C)**, E9.25 **(D–F)**, E10 **(G–I)**, and E15 **(J–L)** embryos. A temporal increment of 5-MeC-im is demonstrated from E8.25 to E9.25. An anteroposterior (AP) gradation (indicated by intensity grading with ''+'' sign) is shown in the hindbrain > forebrain > caudal spinal cord in E8.25, E9.25, and E10. This is in agreement with the gradation of the neural tube maturation and neural tube fusion that are initiated from the midbrain and hindbrain and propagated rostrally to the frontal pole and caudally to the spinal cord. Also, a ventral to dorsal gradation (decrease) is shown in panels **(A, B, E, G,** and **H)**. At E15, the 5-MeC-im appears in almost all cells shown in the cortex **(K, L)** and hippocampus **(J)**. The level of the sections in the neural tube of each age is illustrated in the left column with a correspondent letter in lower case. The division of dorsal/ventral neural tube and the neural crest (NC) region is exemplified in **(H)**. The scale of ''+'' according to H-score was used to indicate the overall regional staining density. NT, neural tube region; V and D, ventral to dorsal direction in the neural tube; hipp, hippocampus. Scale bar: A, B, C, E, F = 100μm, D = 100μm, G–K = 100μm, L = 100μm.

cells, adopted initial morphologic change, and embarked on migration (Fig. 2A). Later, it spread and diffused throughout the nucleus in further differentiated cells in the neural tube (Fig. 2B and C). A population distribution pattern in the neural tube was also evident. At E8.25, the 5-MeC-im appeared mosaic in the neural tube primodium (Fig. 1A–C). By E9.25, it had clear ventral to dorsal, as well as neural axial, patterns in the embryos (Fig. 1D–F). It first appeared at the ventral aspect of the neural tube, increased over age toward the dorsal aspect from E9.25 on, and reached the roof of the neural tube by E10 to E15 (Fig. 1G–L). Axial wise, the earliest and highest 5-MC-im density appeared in the midbrain and rhombomere level. A bidirectional progressive increase extended rostrally toward cortices and caudally toward the caudal neural tube throughout E8.25 to E10 (Fig. 1A–I). The 5-MeC-im distribution in the neural crest cells is parallel to that of the neural tube at the temporal pattern, which includes migrated cells in the pharyngeal arches and dorsal root ganglia in the spinal cord level. Thus, there are two gradational distributions of 5-MeC-im which also progress between E8.25 and E15.

The MBD1-im is distributed similarly to 5-MeC-im (Fig. 2D–F, and Fig. 3) but differently over the course of time. No obvious MBD1-im was seen in E8.5 at the neu-

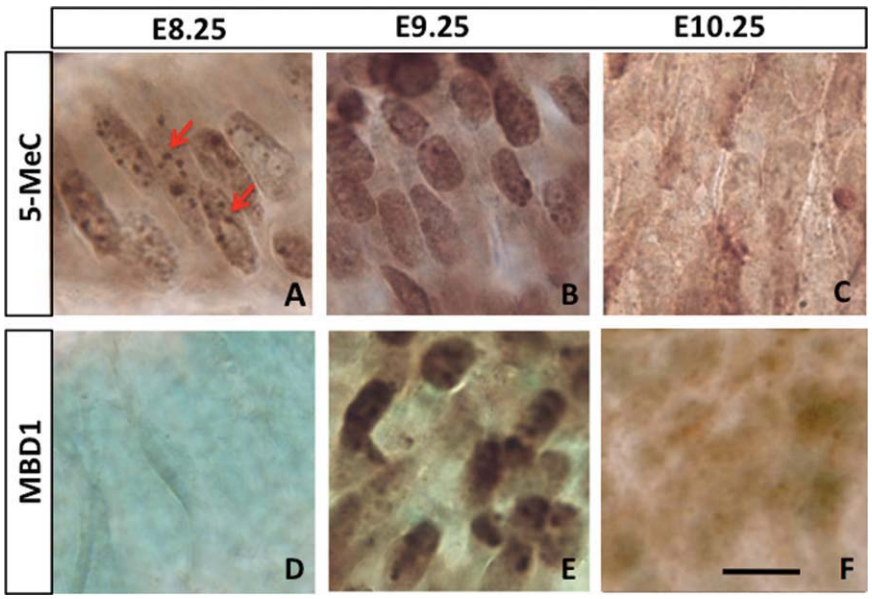

Figure 2. High-magnification microscopic section shows 5-MeC-im **(A–C)** and methylation binding domain 1 (MBD1-im) cells **(D and E)** in E8.25, E9.25, E10.25 embryos. *Arrow*: 5-MeC-im punctate (consolidated) form in the nucleus at E8.25. Scale bar: All = 10μm.

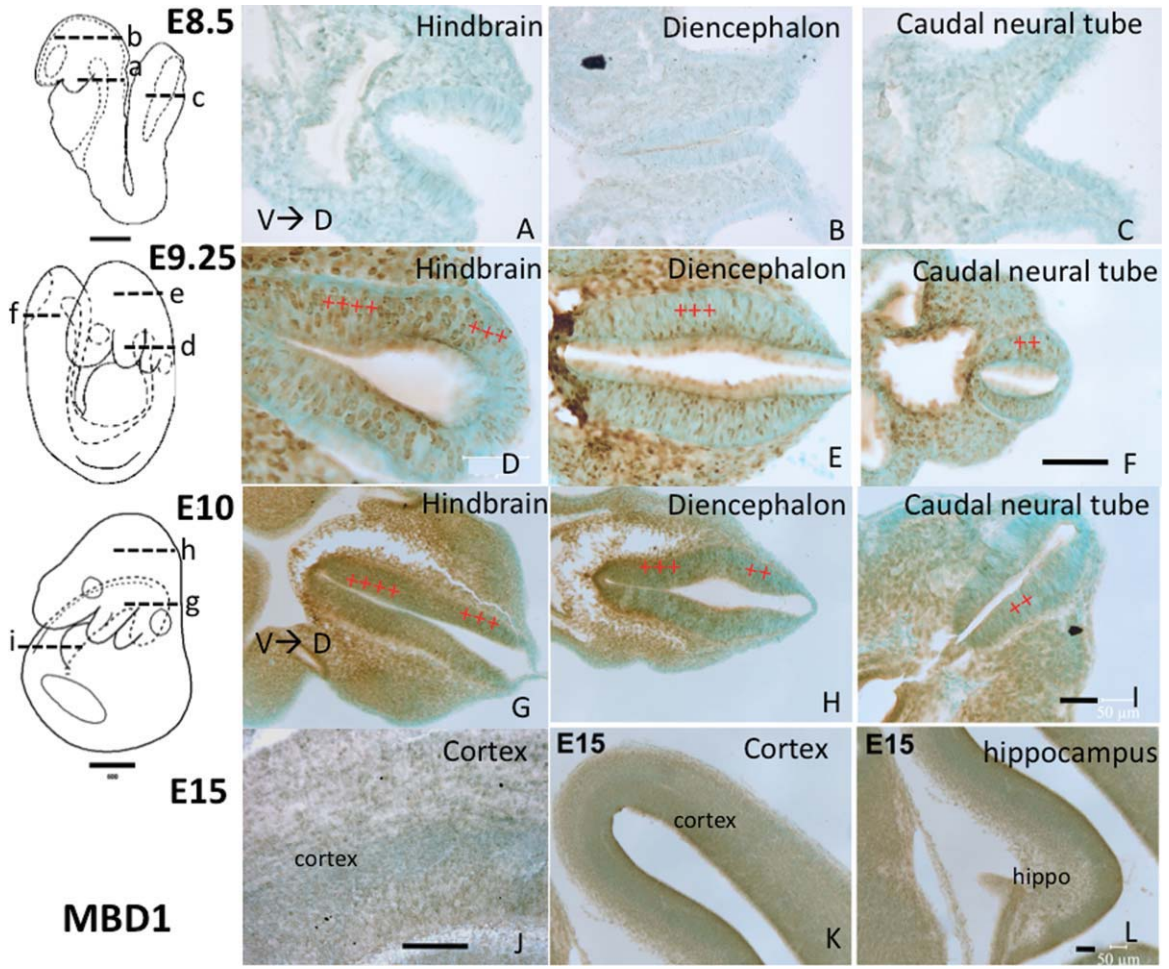

Figure 3. The MBD1-im is similarly distributed as that of 5-MeC-im at E9.25 **(D–F)** and E10 **(G–I)**, but is absent in E8.5 **(A–C)**. A mosaic pattern of MBD1-im distribution is seen at E9.25. At E10 the anterioposterial and ventrodorsal gradation are discernable (indicated by intensity levels shown with '' +'' sign), where hindbrain **(G)** > diencephalon **(H)** > caudal spinal cord **(I)**; and ventral neural tube >dorsal neural tube. At E15 the MBD1-im appears in almost every cell but reduces greatly in intensity as shown in the cortex **(J, K)** and hippocampus (Hipp, L). Scale bar: A–F = 100μm, G–I = 100μm, J = 100μm, K, L = 50μm. The level of the sections in the neural tube of each age is illustrated in the left with correspondent letter in lower case. V and D, ventral to dorsal direction in the neural tube.

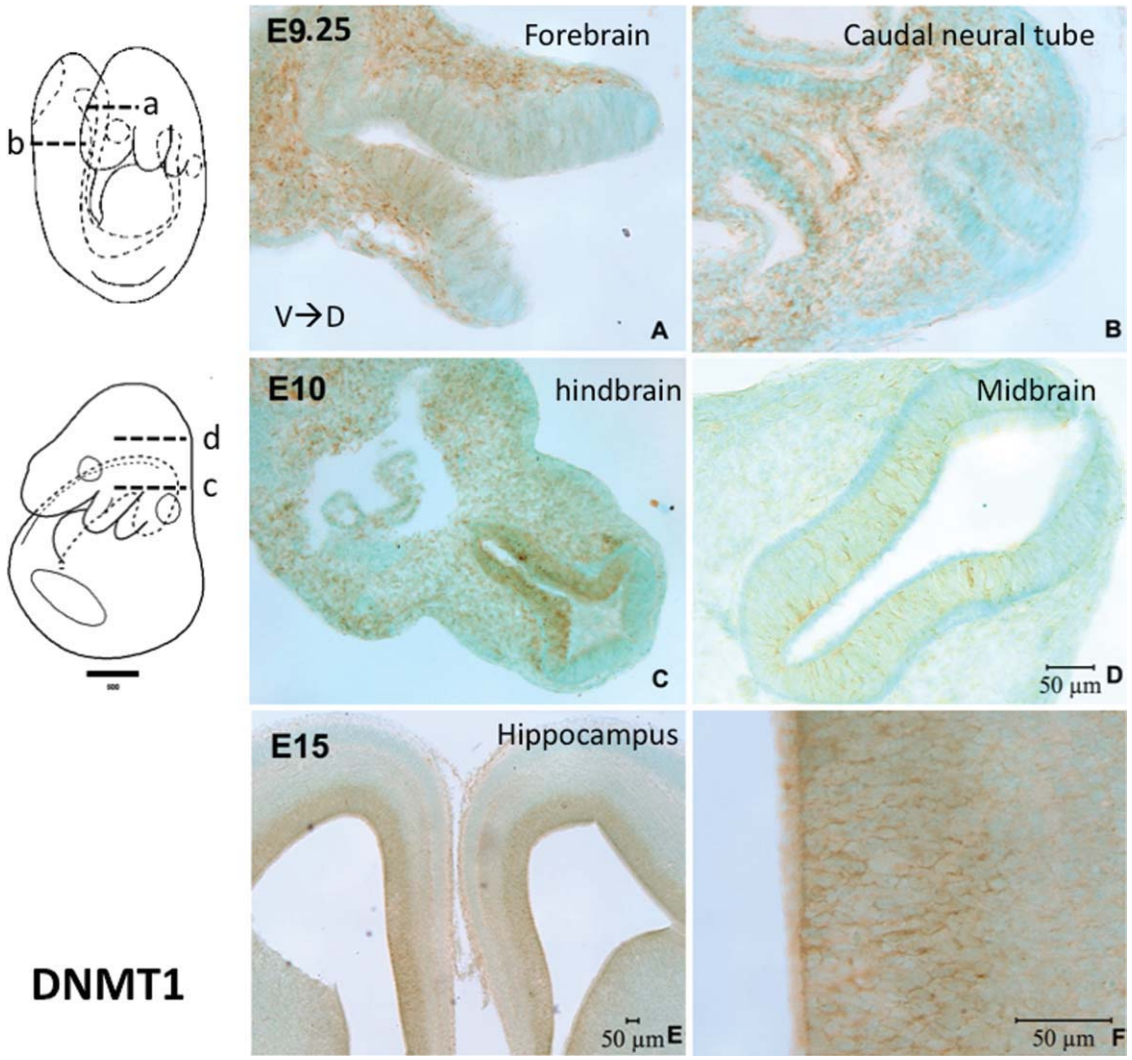

Figure 4. The temporal development and spatial distribution of DNA methyl transferase 1 (DNMT1). The DNMT1 is very lightly stained in the neural tube at E9.25 **(A, B)** but increases significantly in the ventral aspect of the neural tube at E10 **(C, D)**. Its staining is reduced at E15 and remains mostly in the subventricular region in the forebrain **(***arrows*, **E)**. The intracellular distribution is translocated to the cytoplasm in both the high and low expressed cells at E15 **(E, F)**. Scale bar: A–D = 50μm, E = 50μm, F = 50μm. V and D, ventral to dorsal direction in the neural tube.

ral tube primodium about a half day to a day behind 5-MeC (Fig. 2D). It appeared as a punctate form at E9.25 (Fig. 2E) and spread shortly after and far into E10 (Figs. 2F and 3G–I). At the population level, a mosaic pattern of distribution was seen at E9.25 and turned into a similar ventral to dorsal pattern (as 5-MeC-im) with incremental gradation after E9.25 (Fig. 3D–F). By E15, the MBD1-im was diffused within the nucleus and throughout dorsal and ventral aspects similar to that of 5-MeC-im (Fig. 3J–L). The axial bidirectional distribution is also similar to that of 5-MeC-im from E8.25 to E15.

The DNMT1, which adds methylation to semimethylated DNA (maintenance methylation) is closely associated with that of 5-MeC-im with clear ventral to dorsal, as well as axial, distribution patterns. It is also associated with the temporal progression through gestation E9.25 to E10 (Fig. 4). There are, however, a number of differences between the two marks in which DNMT1 (1) lacked a punctate form distribution at E9.25 (Fig. 4A and B); (2) was low at E15 in the differentiated neural cells, but remained high in the undifferentiated regions near the ventricle (e.g., subplate; Fig. 4E and F), which was highly correlated with the pattern of the progenitor layer in the neural tube. Furthermore, at this stage, most of the DNMT1 were translocated into cytoplasm (Fig. 4E and F). The reason for the active translocation of DNMT1 into cytoplasm at the E15 stage is unclear. It is interesting that the cytoplasmic translocation of DNMT1 was also observed during traumatic brain injury, which is also highly expressed in the cortical subplate that coincides with nestin-positive cells (Lundberg et al., 2009).

Distribution of Differentiation Markers

There is a maturation gradation of the neural tube at the cellular level as indicated by neural stem cell and dif-

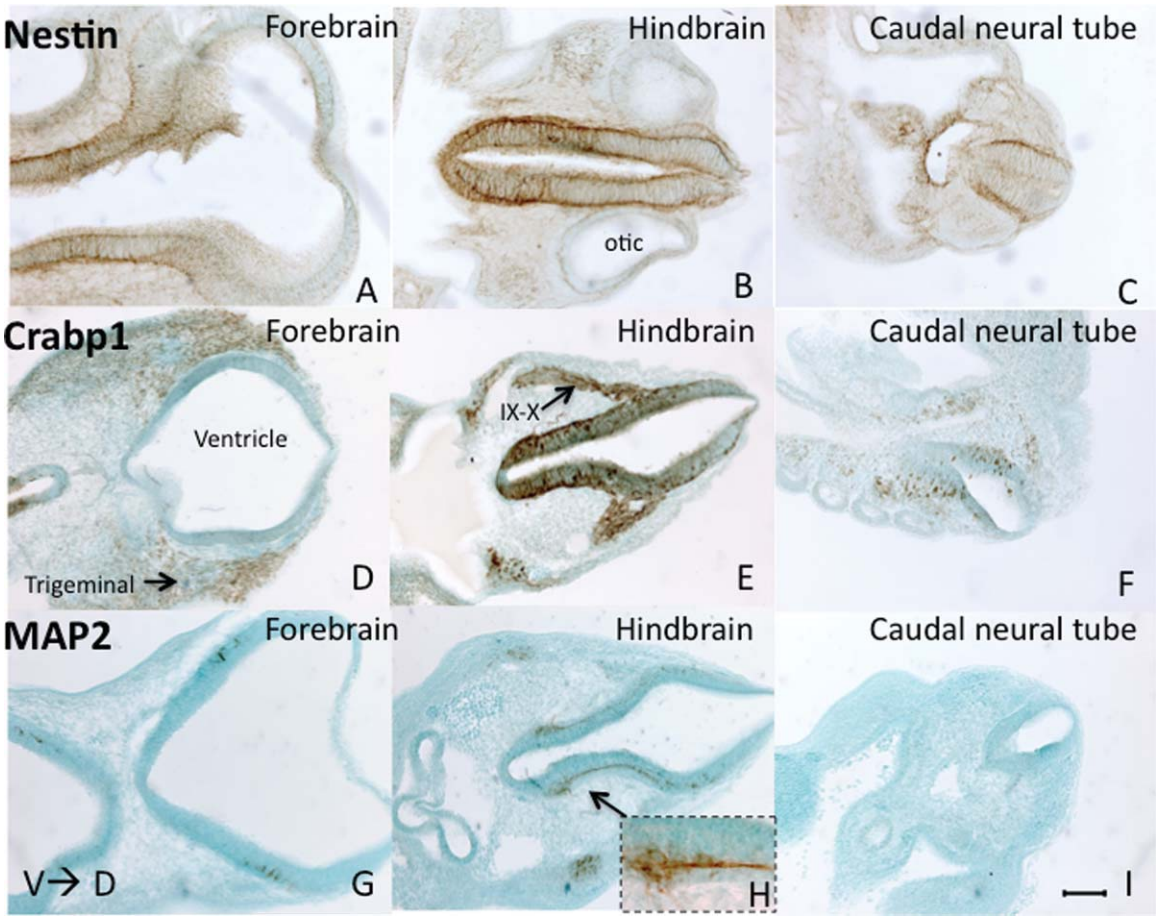

Figure 5.

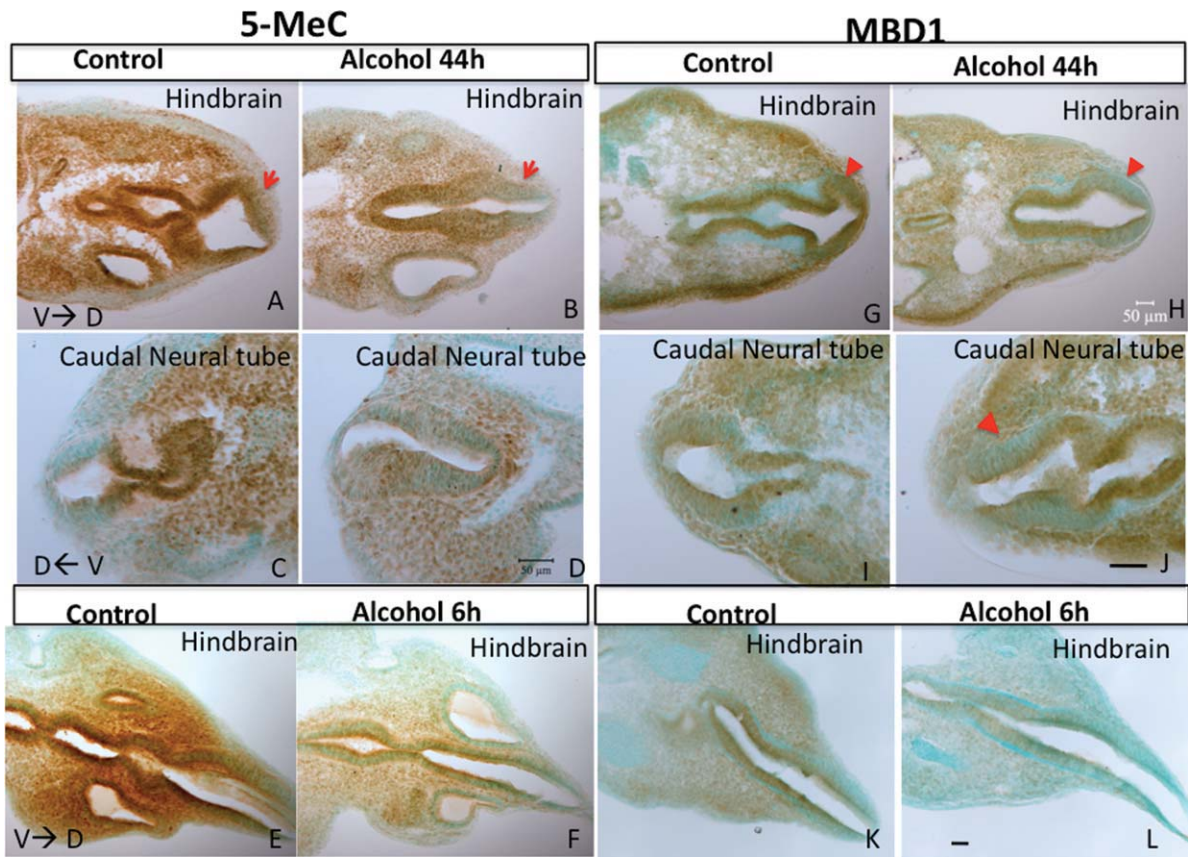

Figure 6.

ferentiating markers, nestin, Crabp1, and MAP2 (Fig. 5). Nestin, a neural progenitor cell-specific marker, is abundantly expressed in the neural tube at E10.25. The nestin-im showed a clear ventral-dorsal density and axial pattern in the neural tube in which the ventral > dorsal neural tube and the hindbrain > forebrain > caudal neural tube. At E10.25, MAP2 already showed in the neural tube at the level of the midbrain and rhombomere, but it was absent in the caudal neural tube. The MAP2-im was shown mostly at the ventral edge of the neural tube, located at the outer segment of the neural tube. The crabp1-im in E10.25 embryos were found in the neural crest cells migrating out on either side of the neural tube at the midbrain and hindbrain levels as well as at the truncal dorsal root ganglia. There was less or no crabp1-im in the caudal neural tube. These markers demonstrated a spatial gradation of differentiation or maturation (e.g., mature neurons appeared earlier in the ventral than in the dorsal aspect of the neural tube and earlier in the midbrain to hindbrain than in the forebrain and caudal neural tube).

Effect of Alcohol Exposure

On embryo development. Among all cultured embryos, more than 95% maintained active heartbeats and blood circulation. Only the embryos with active heartbeats and blood circulation were used for analysis. Besides the apparent decreased vascularization on the yolk sac, the major effect of alcohol to the embryo's development is the neural tube formation. Both delay and abnormality occurred during the current alcohol treatment paradigm. In 44 hours, alcohol treatment (Table 2), major developmental delay was found in the neural tube, forebrain, hindbrain, optic system, branchial arch, heart, forelimb, and hindlimb. In addition, the scores were significantly compromised in the alcohol group as compared to those of the control group.

On DNA methylation. Apparently subjected to the environmental input, the DNA methylation in the developing nervous system was suppressed by alcohol during neurulation. We found in 6 hours, the alcohol group 5-MeC-im were reduced at the end of the culture period at ~ E10 (E8.25+2), particularly at the dorsal neural tube throughout the neural axial level, and at the heart (Table 3A, Fig. 6E and F). In 44 hours, in the alcohol group the 5-MeC-im were reduced in both the dorsal neural tube (at the hindbrain and forelimb levels) and the ventral neural tube (throughout the neural axis from the forebrain level down to the forelimb level; Table 3B, Fig. 6A–D). Thus, binge-like alcohol exposure delays the DNA methylation toward the dorsal aspect of the neural tube at the rostral neural tube. Longer alcohol exposure affects both the dorsal and ventral neural tube and the neural axis (except for the caudal neural tube which had not been highly methylated at the age of analysis).

On DNA methylation-binding protein. The programmed distribution of DNA methylation-binding protein indicated by MBD1-im in the dorsal neural tube was also repressed by 6 hours of alcohol exposure at the hindbrain and heart levels (Table 3C, Fig. 6K and L). Longer alcohol exposure for 44 hours reduced MBD1-im in both the dorsal neural tube and ventral neural tube (Fig. 6G–J).

Effect of 5-AZA Treatment

The embryo growth was retarded in the 44 hour 5-AZA treated group in key organs and neural tube including heart, forebrain, caudal neural tube, similar to those of alcohol treated (Table 2). The total growth score was significantly lower in the treated than the control. The embryo growth was not significantly retarded in the short treatment of 6 hour 5-AZA (Table 2), which indicates that a lasting suppression DNA methylation more than hours, is required to retard the embryonic growth.

DISCUSSION

Progression of DNA Methylation through Development

This report showed, for the first time, the distribution of cellular DNA methylation in the gestational stage of embryonic development in the mouse. A number of our findings are critical to the understanding of whether or not DNA methylation is in position to play a role in embryonic development. In this report, our observation is focused on the nervous system. The first key feature we found was that the DNA methylation marks (e.g., 5-MeC, MBD1, and DNMT) appeared in a ventral (high) to dorsal (low) gradation. This coincided with the maturation gradation of neural tube patterning in which ventral neural specification precedes that of the dorsal. This was indicated by nestin, Map2, and Crabp staining which represent the maturation of neurons and neural crest cells (Marsden et al., 1996; Kleinjan et al., 1997; Jin et al., 2009). A similar coincidence was found in the neural axis, in which gradation of maturation and DNA methylation marks is peaked at midbrain to hindbrain and pro-

Figure 5. Distribution of differentiation markers nestin **(A–C)**, Crabp1 **(D–F)**, microtubule-associated protein 2 (MAP2) **(G–I)** in ~E10 embryos. All embryos were coronal sectioned and oriented dorsal aspect to the right. An axial gradation of nestin expression can be seen in the neural tube, in which hindbrain> forebrain> caudal neural tube. The crabp1 is shown mostly at hindbrain, which give rise to cranial nerve IX and X, and decreases rostrally and caudally. MAP2 appeared along the ventral side of the hindbrain, is less in forebrain, and is absent in caudal neural tube. H: a high magnification of MAP2-im at the marginal zone of neural tube is shown in the box. Scale bar: All = 100μm.

Figure 6. Effects of 44 hour or 6 hour alcohol treatment on 5-MeC-im **(A–F)** and MBD1-im **(G–L)** examined at E10 (E8.25+2). The 44-hour alcohol exposure (first row) reduced 5-MeC-im at the end of culture approximately. Greater decrease of 5-MeC-im staining is found in the dorsal region (*arrows*) in the rostral neural tube **(A vs. B)** and the caudal neural tube **(C vs. D)**. A similar effect upon alcohol exposure was found in MBD1-im, with a major decrease in the dorsal (*arrowhead*, **G vs. H)** and caudal neural tube **(I vs. J)**. Scale bars: A, B, E, F, G, H, K, L = 50μm, C, D, I, J = 50μm. The hindbrains of coronal-section (1st and 3rd rows) were oriented dorsal aspect to the right (V–>D); the caudal neural tubes (2nd row) were oriented dorsal aspect to the left (D–>V).

Table 2
Morphology scoring of cultured embryos at 44-hour alcohol exposure, 6-hour, and 44-hour AZA exposure and their controls

Region	Control	Alcohol/44 hours	Control	AZA/44 hours	Control	AZA/6 hours
Heart	4.84 ± 0.07	4.17 ± 0.15†	4.83 ± 0.09	3.93 ± 0.22*	4.42 ± 0.18	4.26 ± 0.18
Caudal neural tube	4.77 ± 0.09	4.07 ± 0.14†	4.94 ± 0.06	4.21 ± 0.24*	4.58 ± 0.16	4.26 ± 0.23
Hindbrain	4.77 ± 0.08	4.17 ± 0.15*	4.83 ± 0.09	4.57 ± 0.14	4.84 ± 0.09	4.47 ± 0.16
Midbrain	4.65 ± 0.09	4.14 ± 0.15	4.94 ± 0.06	4.36 ± 0.23	4.95 ± 0.05	4.53 ± 0.19
Forebrain	4.81 ± 0.07	4.10 ± 0.15†	5.00 ± 0.00	4.21 ± 0.21†	4.79 ± 0.10	4.47 ± 0.18
Otic system	4.10 ± 0.11	3.79 ± 0.09	4.28 ± 0.11	4.14 ± 0.14	4.37 ± 0.11	4.11 ± 0.07
Optic system	4.71 ± 0.09	4.17 ± 0.13*	4.67 ± 0.11	4.14 ± 0.21	4.79 ± 0.12	4.47 ± 0.18
Olfactory system	0.61 ± 0.09	0.52 ± 0.09	0.67 ± 0.11	0.50 ± 0.14	0.47 ± 0.12	0.47 ± 0.12
Branchial bars	2.87 ± 0.06	2.69 ± 0.09	2.94 ± 0.06	2.57 ± 0.17	2.95 ± 0.05	2.79 ± 0.10
Maxillary process	2.84 ± 0.07	2.62 ± 0.10	2.89 ± 0.08	2.71 ± 0.13	2.79 ± 0.10	2.53 ± 0.12
Mandibular process	2.06 ± 0.06	2.00 ± 0.05	1.94 ± 0.10	1.93 ± 0.07	1.95 ± 0.05	1.84 ± 0.09
Forelimb	1.77 ± 0.08	1.34 ± 0.10*	1.78 ± 0.10	1.29 ± 0.13	1.63 ± 0.11	1.47 ± 0.12
Hindlimb	1.03 ± 0.12	0.69 ± 0.11	1.44 ± 0.12	1.00 ± 0.15	1.32 ± 0.11	1.21 ± 0.14
Total score	43.84 ± 0.44	38.48 ± 0.83†	45.17 ± 0.39	39.57 ± 1.30†	43.84 ± 0.62	40.89 ± 1.12

Mann–Whitney *U* analysis used.
*p value < 0.0038.
†p value < 0.0007 compare to control. Forty-four hour Alcohol Control n = 31; Alcohol n = 29.
Forty-four hour AZA Control n = 18; AZA n = 14.
Six hour AZA Control n = 19; AZA n = 19.
The morphology scores for 6-hour alcohol treatment embryos were shown in Chen et al., 2011.
AZA, azacytidine.

gressed bidirectionally to the forebrain and caudal neural tube. It may be argued whether or not the DNA methylation is a guiding regulator for or a byproduct of developmental progression. Supporting evidence indicates that (disrupted) DNA methylation may not be a silent byproduct of (delayed) growth, but rather an upstream factor that regulates gene transcription, which affects development. First, inhibition of DNA methylation has been known to affect hematopoietic stem cell fate (Milhem et al., 2004) and proliferation and differentiation of germ cells in testis (Raman and Narayan, 1995). We previously demonstrated that (1) DNA methylation and the MBD1 in neural stem cells were dynamically changed according to the state of stem cell differentiation, and (2) treatment with 5-AZA prevented the neural stem cell from migration and differentiation (Singh et al., 2009). Five-AZA is known to inhibit DNMTs and DNA methylation, can cause DNA damage, and potentially affects cell proliferation; it has been reported to cause similar deterrence of differentiation (Jones et al., 1983; Christman, 2002; Ghoshal et al., 2005; Singh et al., 2009). We have now provided additional evidence to demonstrate that alteration of DNA methylation per se can lead to distinct embryonic growth retardation. In this study, under a similar embryo growth paradigm, we demonstrated that inhibiting DNA methylation during neurulation led to embryonic growth retardation. Mechanistically, the DNA-methylation has been demonstrated to modify the transcription of genes (e.g., DNA methylation status is closely linked to the chromatin structure of the Oct4 gene necessary for the pluripotency of many stem cells; 5-AZA by suppressing DNA methylation caused the activation of the Oct4 gene (Hattori et al., 2004). Finally, DNA methylation is known for mediating tissue specification; cell-type-specific genes including receptors, hormones, and intracellular signaling molecules with tissue-specific differentially methylated regions are methyl-

Table 3A
The 5-MeC staining in neural tube of E8.2 + 2 cultured embryos

Neural tube at level of	6-hour	Ventral	Dorsal
Forebrain	Control	148.67 ± 16.80	109.55 ± 17.11
	Alcohol	123.57 ± 15.08	96.74 ± 16.23*
Hindbrain	Control	150.18 ± 15.41	116.70 ± 13.31
	Alcohol	124.26 ± 10.85	87.46 ± 8.31*
Heart	Control	144.80 ± 17.86	112.37 ± 10.32
	Alcohol	120.06 ± 6.47	89.16 ± 6.56*
Forelimb	Control	136.97 ± 9.90	109.66 ± 3.76
	Alcohol	110.32 ± 12.35	85.79 ± 12.31

Six-hour alcohol treatment.
N = 3, *$p < 0.05$.
Data presented as mean ± SEM.
5-MeC, 5-methylcytosine.

Table 3B
The 5-MeC staining in E8.2 + 2 cultured embryos

Neural tube at level of	44-hour	Ventral	Dorsal
Forebrain	Control	149.79 ± 5.33	117.04 ± 5.34
	Alcohol	129.60 ± 7.66*	110.32 ± 7.66
Hindbrain	Control	147.90 ± 4.36	129.71 ± 3.77
	Alcohol	131.23 ± 5.55*	112.95 ± 7.72*
Heart	Control	146.78 ± 7.60	127.37 ± 6.47
	Alcohol	132.59 ± 4.63†	115.19 ± 8.03
Forelimb	Control	138.78 ± 8.78	121.04 ± 8.78
	Alcohol	124.58 ± 8.36†	114.63 ± 9.08*

Forty-four-hour alcohol treatment.
N = 4, *$p < 0.05$, †$p < 0.01$ compare to control.
Data presented as mean ± SEM.
5-MeC, 5-methylcytosine.

Table 3C
MBD1 staining in E8.2 + 2 cultured embryos

Neural tube at level of	6-hour	Ventral	Dorsal
Forebrain	Control	148.75 ± 8.00	93.66 ± 2.87
	Alcohol	147.31 ± 9.20	97.42 ± 14.71
Hindbrain	Control	173.48 ± 5.70	134.88 ± 2.25
	Alcohol	175.78 ± 1.13	147.25 ± 4.39*
Heart	Control	156.98 ± 2.70	127.29 ± 3.35
	Alcohol	145.37 ± 11.77	90.27 ± 11.45*
Forelimb	Control	150.36 ± 9.62	111.20 ± 5.42
	Alcohol	145.68 ± 7.98	112.43 ± 2.67

Six-hour alcohol treatment.
N = 4, *$p < 0.05$.
Data presented as mean ± SEM.
MBD1, methylation binding domain 1.

ated for permissive expression at early developmental stages (Ohgane et al., 2008).

The second interesting feature is the dynamic intracellular distribution of DNA methylation over age or state of differentiation. The DNA methylation mark appeared not by random but in the spatial and temporal pattern which coincides with the pattern of cell differentiation and the progression of development in the neural tube and neural crest. At early gestation E8.25, in which commitment to neural stem cells prevails, the highlight of DNA methylation (or hypermethylation) within the nuclei of cells undergoing differentiation was consolidated and aggregated as a punctuate; this represents a remodeling of chromatin along the chromosome. Given the general repressive nature of DNA methylation on DNA transcription, this would indicate a potential turn-off of clusters of genes (e.g., pan-stem cells genes for renewal and proliferation). A many DNA free of CpG methylation (or hypomethylated) and not associated with methylated DNA aggregate would likely open for transcription (e.g., neural stem cell genes or early neural genes would contribute to the initiation of neurulation). The dynamics of the DNA methylation at the wake of neural stem cell differentiation were also evident at the gene level. We have demonstrated that during neural stem cell differentiation from the quiescent stage, many genes undergo DNA methylation change (Zhou et al., 2011); like a program, many moderately methylated genes became hypermethylated as well as hypomethylated during the initiation of differentiation.

Third, we found a dormant stage of DNA methylation. Noticeably, throughout gestation E8.5 to 10 stages, there was a population of cells that was either low in DNA methylation or hypomethylated. The understanding of DNA methylation transmission from mother to daughter cells is that it occurs at the stage of DNA duplication which is mediated by DNMT1 and aided by proliferating cell nuclear antigen at the loading clamp of the DNA replication folk (Ng and Gurdon, 2008; Lange and Schneider, 2010); it would take place immediately after cell division. However, our observation of low to no DNA methylation in a subpopulation of cells indicated that the absence of maintenance or de novo DNA methylation can remain for a lengthy period of time in which the precursor cells wait for their turn for differentiation (e.g., dorsal or caudal neural tube at E8 or E9). However, it cannot be ruled out that these cells may lack 5-MeC-im as their chromosomes were highly packed. Hence, they were less accessible for detection by the anti-5-MeC antibodies or were inaccessible for transcription (other than for housekeeping genes). Our observation on a similar pattern of low distribution (to 5-MeC-im) of the DNA methylation enzyme, DNMT1, in the dorsal and caudal aspects of the neural tube at a similar gestational stage, supports the first premise. It is agreeable, in either premise, that the cells that lack or are low in 5-MeC-im were those undifferentiated or inert cells in the least mature regions of the neural tube (e.g., caudal neural tube, or dorsal aspect of neural tube). Our point is that there are multiple cycles of DNA methylation through the lengthy developmental processes after the erasure at fertilization through early blastocyst; many daughter cells may use a low methylation state to maintain their multipotency as they wait their turn for differentiation.

The MBD1 has very similar dynamics to the 5-MeC in the above features. It probably does so to collaboratively regulate the transcription. The DNA methylation, other than rendering the conformation change of DNA, often requires a reader for its function. As a major methyl CpG-binding protein, MBD1 recruits a repressor complex or various DNA-binding protein, including the histone of repressive code (e.g., trimethyl Histone 3 lysine-9, me3H3K9; Ng et al., 2000; Fujita et al., 2003a; Fujita et al., 2003b). It also mediates transcriptional repression and other functions. It is interesting that the peak of the MBD expression was slightly behind that of 5-MeC-im in most of the cells in the neural tube. The additional delay or reduction caused by alcohol would significantly affect the function. The dynamic relationship between DNA methylation and its binding partner is likely an essential program for multipotent precursor cells that embark on migration or turn on differentiation.

DNA Methylation Program and Altered State

Prenatal alcohol exposure has been demonstrated to cause FASD; the mechanism behind the cause is unclear and likely to be multiple. A major event of the alcohol on FASD is an overall delay in development, which is again evident in our closely controlled test system in the embryonic culture in this and a previous study (Ogawa et al., 2005). In this study, we demonstrated growth retardation (Table 2) in the forebrain, hindbrain, heart, caudal neural tube, optic vesicle, and limbs. In addition, alcohol exerted a potent and long-lasting effect on DNA methylation and the MBD1 level. A shorter alcohol exposure equivalent to binge drinking (6 hours) delayed the DNA methylation program in the dorsal neural tube at the hindbrain, forebrain, and truncal (heart) level of the neural tube at the end of the 2-day culture. Longer exposure (44 hours) like chronic drinking delayed both the ventral and dorsal neural tube at multiple levels along the neural tube axis. The effect of DNA methylation is further supported by the 5-AZA treatment study which demonstrated that inhibiting DNA methylation >40 hours during neurulation led to embryonic growth retardation in regions similar to that of the alcohol treated. Furthermore, the DNA methylation program delay paralleled the developmental delay of the neural tube in a spatial and temporal pattern. The effect of DNA methylation change in the dorsal neural tube can lead to regional developmental delay or neural tube defect. The effect of

DNA methylation changes in the ventral neural tube is likely to be more profound. Many key genes encoding important morphogen and neurotrophic factors, which are important for differentiation and growth, are located in the floor plate of the neural tube (e.g., the sonic hedgehog and neurotrophic factor fibroblast growth factor; Ye et al., 1998; Dessaud et al., 2008). Temporally, the long alcohol exposure (44 hours) resulted in more severe growth retardation than the shorter (6 hours) alcohol exposure in comparing this and previous studies (Chen et al., 2011). The longer inhibition of DNA methylation also resulted in greater growth delay (Table 2). Finally, the alteration of cellular DNA methylation by alcohol has been demonstrated in the gene level in which genes known to play roles in cell cycle, growth, apoptosis, cancer, and in many genes associated with olfaction were affected (Liu et al., 2009).

In summary, DNA methylation is progressively modified with distinct temporal and spatial patterns at the stage of neurulation. An increase of DNA methylation, including DNA methylation (5-MeC), DNA methylation-binding protein 1 (MBD1), and the enzyme which maintains DNA methylation (DNMT1), coincides with temporal maturation. There is (1) a bidirectional anterioposterial gradation peak at midbrain to the hindbrain of DNA methylation along the neural tube and (2) a dorsoventral gradation, which coincides with the maturation gradation and may mediate patterning of the neural tube. Known to delay embryo development, alcohol abuse, which in part shares a common effect with the DNA methylation inhibitor, delays the DNA methylation program. A causal hypothesis in which alcohol affects epigenetic progression to delay the embryonic development is a compelling warrant for further investigation.

ACKNOWLEDGMENTS

We thank Ms. Lijun Ni for technical support on embryonic culture.

REFERENCES

Amir RE, Van den Veyver IB, Wan M, et al. 1999. Rett syndrome is caused by mutations in X-linked MECP2, encoding methyl-CpG-binding protein 2. Nat Genet 23:185–188.

Bartolomei MS. 2003. Epigenetics: role of germ cell imprinting. Adv Exp Med Biol 518:239–245.

Bird AP. 1987. CpG islands as gene markers in the vertebrate nucleus. Trends Genet 3:342–347.

Boehm SL 2nd, Lundahl KR, Caldwell J, Gilliam DM. 1997. Ethanol teratogenesis in the C57BL/6J, DBA/2J, and A/J inbred mouse strains. Alcohol 14:389–395.

Brown NA, Fabro S. 1981. Quantitation of rat embryonic development in vitro: a morphological scoring system. Teratology 24:65–78.

Chen Y, Ozturk NC, Ni L, et al. 2011. Strain differences in developmental vulnerability to alcohol exposure via embryo culture in mice. Alcohol Clin Exp Res [Epub ahead of print].

Cheng LC, Tavazoie M, Doetsch F. 2005. Stem cells: from epigenetics to microRNAs. Neuron 46:363–367.

Christman JK. 2002. 5-Azacytidine and 5-aza-2′-deoxycytidine as inhibitors of DNA methylation: mechanistic studies and their implications for cancer therapy. Oncogene 21:5483–5495.

Cravo ML, Camilo ME. 2000. Hyperhomocysteinemia in chronic alcoholism: relations to folic acid and vitamins B(6) and B(12) status. Nutrition 16:296–302.

Dessaud E, McMahon AP, Briscoe J. 2008. Pattern formation in the vertebrate neural tube: a sonic hedgehog morphogen-regulated transcriptional network. Development 135:2489–2503.

Detre S, Saclani Jotti G, Dowsett M. 1995. A ''quickscore'' method for immunohistochemical semiquantitation: validation for oestrogen receptor in breast carcinomas. J Clin Pathol 48:876–878.

Fujita N, Watanabe S, Ichimura T, et al. 2003a. MCAF mediates MBD1-dependent transcriptional repression. Mol Cell Biol 23:2834–2843.

Fujita N, Watanabe S, Ichimura T, et al. 2003b. Methyl-CpG binding domain 1 (MBD1) interacts with the Suv39h1-HP1 heterochromatic complex for DNA methylation-based transcriptional repression. J Biol Chem 278:24132–24138.

Garro AJ, McBeth DL, Lima V, Lieber CS. 1991. Ethanol consumption inhibits fetal DNA methylation in mice: implications for the fetal alcohol syndrome. Alcohol Clin Exp Res 15:395–398.

Ghoshal K, Datta J, Majumder S, et al. 2005. 5-Aza-deoxycytidine induces selective degradation of DNA methyltransferase 1 by a proteasomal pathway that requires the KEN box, bromo-adjacent homology domain, and nuclear localization signal. Mol Cell Biol 25:4727–4741.

Giknis ML, Damjanov I, Rubin E, et al. 1980. The differential transplacemental effects of ethanol in four mouse strains. Neurobehav Toxicol 2:235–237.

Goodlett CR, Horn KH, Zhou FC. 2005. Alcohol teratogenesis: mechanisms of damage and strategies for intervention. Exp Biol Med (Maywood) 230:394–406.

Hamid A, Wani NA, Kaur J. 2009. New perspectives on folate transport in relation to alcoholism-induced folate malabsorption–association with epigenome stability and cancer development. FEBS J 276:2175–2191.

Hansen RS, Wijmenga C, Luo P, et al. 1999. The DNMT3B DNA methyltransferase gene is mutated in the ICF immunodeficiency syndrome. Proc Natl Acad Sci U S A 96:14412–14417.

Hattori N, Nishino K, Ko YG, et al. 2004. Epigenetic control of mouse Oct-4 gene expression in embryonic stem cells and trophoblast stem cells. J Biol Chem 279:17063–17069.

Haycock PC. 2009. Fetal alcohol spectrum disorders: the epigenetic perspective. Biol Reprod 81:607–617.

Hoffman F. 1975. Generalized depressants of the central nervous system. In: Hoffman F, Hoffman A, editors. A handbook of drug and alcohol abuse. New York: Oxford University Press. pp 95–128.

Jin Z, Liu L, Bian W, et al. 2009. Different transcription factors regulate nestin gene expression during P19 cell neural differentiation and central nervous system development. J Biol Chem 284:8160–8173.

Jones PA, Taylor SM, Wilson VL. 1983. Inhibition of DNA methylation by 5-azacytidine. Recent Results Cancer Res 84:202–211.

Kafri T, Ariel M, Brandeis M, et al. 1992. Developmental pattern of gene-specific DNA methylation in the mouse embryo and germ line. Genes Dev 6:705–714.

Kiefer JC. 2007. Epigenetics in development. Dev Dyn 236:1144–1156.

Kleinjan DA, Dekker S, Vaessen MJ, Grosveld F. 1997. Regulation of the CRABP-I gene during mouse embryogenesis. Mech Dev 67:157–169.

Kondo T. 2006. Epigenetic alchemy for cell fate conversion. Curr Opin Genet Dev 16:502–507.

LaBaume LB, Merrill DK, Clary GL, Guynn RW. 1987. Effect of acute ethanol on serine biosynthesis in liver. Arch Biochem Biophys 256:569–577.

Lange UC, Schneider R. 2010. What an epigenome remembers. Bioessays 32:659–668.

Lindblad B, Olsson R. 1976. Unusually high levels of blood alcohol? JAMA 236:1600–1602.

Liu Y, Balaraman Y, Wang G, et al. 2009. Alcohol exposure alters DNA methylation profiles in mouse embryos at early neurulation. Epigenetics 4:500–511.

Lundberg J, Karimi M, von Gertten C, et al. 2009. Traumatic brain injury induces relocalization of DNA-methyltransferase 1. Neurosci Lett 457:8–11.

Marsden KM, Doll T, Ferralli J, et al. 1996. Transgenic expression of embryonic MAP2 in adult mouse brain: implications for neuronal polarization. J Neurosci 16:3265–3273.

Mason JB, Choi SW. 2005. Effects of alcohol on folate metabolism: implications for carcinogenesis. Alcohol 35:235–241.

McGeer PL, McGeer EG, Nagai T. 1983. GABAergic and cholinergic indices in various regions of rat brain after intracerebral injections of folic acid. Brain Res 260:107–116.

Meshorer E. 2007. Chromatin in embryonic stem cell neuronal differentiation. Histol Histopathol 22:311–319.

Milhem M, Mahmud N, Lavelle D, et al. 2004. Modification of hematopoietic stem cell fate by 5aza 2′deoxycytidine and trichostatin A. Blood 103:4102–4110.

Morgan HD, Santos F, Green K, et al. 2005. Epigenetic reprogramming in mammals. Hum Mol Genet 14 Spec No 1:R47–58.

New DA. 1978. Whole-embryo culture and the study of mammalian embryos during organogenesis. Biol Rev Camb Philos Soc 53:81–122.

Ng HH, Jeppesen P, Bird A. 2000. Active repression of methylated genes by the chromosomal protein MBD1. Mol Cell Biol 20:1394–1406.

Ng RK, Gurdon JB. 2008. Epigenetic inheritance of cell differentiation status. Cell Cycle 7:1173–1177.

Ogawa T, Kuwagata M, Ruiz J, Zhou FC. 2005. Differential teratogenic effect of alcohol on embryonic development between C57BL/6 and DBA/2 mice: a new view. Alcohol Clin Exp Res 29:855–863.

Ohgane J, Yagi S, Shiota K. 2008. Epigenetics: the DNA methylation profile of tissue-dependent and differentially methylated regions in cells. Placenta 29Suppl A:S29–35.

Okano M, Bell DW, Haber DA, Li E. 1999. DNA methyltransferases Dnmt3a and Dnmt3b are essential for de novo methylation and mammalian development. Cell 99:247–257.

Pfeifer GP, Tanguay RL, Steigerwald SD, Riggs AD. 1990. In vivo footprint and methylation analysis by PCR-aided genomic sequencing: comparison of active and inactive X chromosomal DNA at the CpG island and promoter of human PGK-1. Genes Dev 4:1277–1287.

Raman R, Narayan G. 1995. 5-Aza deoxyCytidine-induced inhibition of differentiation of spermatogonia into spermatocytes in the mouse. Mol Reprod Dev 42:284–290.

Shahbazian MD, Zoghbi HY. 2002. Rett syndrome and MeCP2: linking epigenetics and neuronal function. Am J Hum Genet 71: 1259–1272.

Singal R, Ginder GD. 1999. DNA methylation. Blood 93:4059–4070.

Singh RP, Shiue K, Schomberg D, Zhou FC. 2009. Cellular epigenetic modifications of neural stem cell differentiation. Cell Transplant 18:1197–1211.

Surani MA, Hayashi K, Hajkova P. 2007. Genetic and epigenetic regulators of pluripotency. Cell 128:747–762.

Tang HL, Zhu JH. 2007. Epigenetics and neural stem cell commitment. Neurosci Bull 23:241–248.

Tilghman SM. 1999. The sins of the fathers and mothers: genomic imprinting in mammalian development. Cell 96:185–193.

Ueda Y, Okano M, Williams C, et al. 2006. Roles for Dnmt3b in mammalian development: a mouse model for the ICF syndrome. Development 133:1183–1192.

van Maele–Fabry G, Delhaise F, Picard JJ. 1992. Evolution of the developmental scores of sixteen morphological features in mouse embryos displaying 0 to 30 somites. Int J Dev Biol 36:161–167.

Walsh CP, Bestor TH. 1999. Cytosine methylation and mammalian development. Genes Dev 13:26–34.

Wynter JM, Walsh DA, Webster WS, et al. 1983. Teratogenesis after acute alcohol exposure in cultured rat embryos. Teratog Carcinog Mutagen 3:421–428.

Wu H, Coskun V, Tao J, et al. 2010. Dnmt3a-dependent nonpromoter DNA methylation facilitates transcription of neurogenic genes. Science 329:444–448.

Yamazaki T, Yamagata K, Baba T. 2007. Time-lapse and retrospective analysis of DNA methylation in mouse preimplantation embryos by live cell imaging. Dev Biol 304:409–419.

Ye W, Shimamura K, Rubenstein JL, et al. 1998. FGF and Shh signals control dopaminergic and serotonergic cell fate in the anterior neural plate. Cell 93:755–766.

Zhang B, Pan X, Anderson TA. 2006. MicroRNA: a new player in stem cells. J Cell Physiol 209:266–269.

Zhou FC, Balaraman Y, Teng M, et al. 2011. Alcohol alters DNA methylation patterns and inhibits neural stem cell differentiation. Alcohol Clin Exp Res [Epub ahead of print].